© 2021. Published by The Company of Biologists Ltd | Journal of Experimental Biology (2021) 224, jeb223438. doi:10.1242/jeb.223438

RESEARCH ARTICLE

Size, shape and orientation of macro-sized substrate protrusions affect the toe and foot adhesion of geckos

Yi Song[1,2], Jiwei Yuan[1,*], Linghao Zhang[1,*], Zhendong Dai[1,‡] and Robert J. Full[2,‡]

ABSTRACT

Geckos are excellent climbers using compliant, hierarchically arranged adhesive toes to negotiate diverse terrains varying in roughness at multiple size scales. Here, we complement advancements at smaller size scales with measurements at the macro scale. We studied the attachment of a single toe and whole foot of geckos on macroscale rough substrates by pulling them along, across and off smooth rods and spheres mimicking different geometric protrusions of substrates. When we pulled a single toe along rods, the force increased with the rod diameter, whereas the attachment force of dragging toes across rods increased from about 60% on small diameter rods relative to a flat surface to ∼100% on larger diameter rods, but showed no further increase as rod diameter doubled. Toe force also increased as the pulling changed from along-rod loading to across-rod loading. When toes were pulled off spheres, the force increased with increasing sphere diameter as observed for along-rod pulling. For feet with separated toes, attachment on spheres was stronger than that on rods with the same diameter. Attachment force of a foot decreased as rod and sphere size increased but remained sufficient to support the body weight of geckos. These results provide a bridge to the macroscale roughness seen in nature by revealing the importance of the dimension, shape and orientation of macroscale substrate features for compliant toe and foot function of geckos. Our data not only enhance our understanding of geckos' environmental adaptive adhesion but can also provide inspiration for novel robot feet in development.

KEY WORDS: Gecko adhesion, Macro-scale roughness, Distributed toes, Adaptability

INTRODUCTION

Among the legged animals, geckos can agilely maneuver on various terrains in all orientations (Autumn et al., 2006a; Chen et al., 2006; Song et al., 2020a; Wang et al., 2011, 2015) by using their hierarchically arranged, compliant feet which are covered with elaborate hairs or setae (Ruibal and Ernst, 1965). The foot hairs are distally curved and branched (Ruibal and Ernst, 1965), and can only generate adhesion if they are proximally dragged while being pressed against the substrate at the same time (Autumn et al., 2000), resulting in toes possessing high directionality while generating frictional adhesion (Autumn et al., 2006b). Yet, feet with multiple toes are surprisingly capable of generating environment-adaptive forces on diverse terrains varying in roughness at multiple size scales (Russell and Johnson, 2007). Understanding the interactions between geckos' feet and the rough substrates remains a challenge (Higham et al., 2019; Niewiarowski et al., 2019; Russell et al., 2019). If addressed, it could not only assist in explaining gecko behavior and ecology, but also provide more effective inspiration for artificial adhesives (Ge et al., 2007; Gorb et al., 2007; Qu et al., 2008; Sitti and Fearing, 2003) and robot locomotion (Daltorio et al., 2006; Kim et al., 2007; Menon and Sitti, 2006; Unver et al., 2006).

Studies quantifying force production of feet during locomotion have been carried out on smooth surfaces like level ground (Chen et al., 2006), vertical walls (Autumn et al., 2006a; Song et al., 2020a), and even ceilings (Song et al., 2020b; Wang et al., 2015). Investigators have recognized that geckos, and gecko-inspired adhesives can operate on 3D terrains whose roughness varies over multiple spatial scales (Alexander, 2003; Kaspari and Weiser, 2007; Niewiarowski et al., 2019; Russell and Bellairs, 1976; Russell and Johnson, 2007, 2014; Song et al., 2016). The effects of substrate roughness on adhesion have been primarily explored at nano-, micro- and mesoscopic scales (Gillies et al., 2014; Huber et al., 2007; Naylor and Higham, 2019; Niewiarowski et al., 2019; Russell and Higham, 2009; Russell and Johnson, 2007; Stark et al., 2013; Vanhooydonck et al., 2005). As geckos climb microscale rough terrains, their acceleration performance exhibits a clear roughness dependence (Vanhooydonck et al., 2005). During interactions with nanoscale rough substrates, the adhesion of spatulae varies nonlinearly as the substrate roughness (root mean square, RMS) increases from ∼20 nm to ∼2000 nm (Huber et al., 2007). Tests with whole organisms also confirm a nonlinear variation in clinging force on microscale rough surfaces (Pillai et al., 2020). As toes and feet negotiate mesoscopic roughness, the intermediate-sized blood vessels, tendons, muscles and lamellae allow setal fields to further conform to surface irregularities to produce greater forces (Gillies et al., 2014; Russell, 1981, 2002). Nonetheless, lamellae adhere most poorly when the substrate feature is comparable to their length but perform well on substrates with smaller or larger mesoscopic features (Gillies et al., 2014). When geckos behave in their surroundings, the microscale and mesoscale roughness can cause significant reductions in the substrate area available for setae to contact (Russell and Johnson, 2007; Stark et al., 2015). The reduction in effective contact area further results in reducing the acceleration performance of geckos when they climb microscale rough terrain (Vanhooydonck et al., 2005). However, their claws may mitigate these issues (Naylor and Higham, 2019; Zani, 2000) if the undulations are comparable to the size of claw tips (Dai et al., 2002).

The attachment of toes and feet on macroscale rough substrates where claws can be inoperative (Song et al., 2016) is essential for animals operating in natural environments with three-dimensional geometric shapes and protrusions that include rocks, rough tree bark, twigs and branches (Higham and Jayne, 2004; Krause and Fischer, 2013; Schmidt and Fischer, 2010). For geckos, the unique tendinous structures (Abdala et al., 2009) in toes allow their feet to

[1]College of Mechanical and Electrical Engineering, Nanjing University of Aeronautics and Astronautics, 29 Yudao Street, Nanjing 210016, China. [2]Department of Integrative Biology, University of California, Berkeley, CA 94720, USA.
*These authors contributed equally to this work

‡Authors for correspondence (zddai@nuaa.edu.cn; rjfull@berkeley.edu)

Y.S., 0000-0001-9239-5377; Z.D., 0000-0002-1276-7466

Received 29 February 2020; Accepted 17 February 2021

Journal of Experimental Biology (2021) 224, jeb223438. doi:10.1242/jeb.223438

conform to and even grasp large convex shapes with soft toes (Song et al., 2020a) and to adjust the alignment of toes while climbing on perches as the slopes change (Zhuang and Higham, 2016). Russell et al. (2019) recently emphasized that understanding the interaction between the locomotion appendages of geckos and the natural environment remains a necessity to enhance our knowledge of geckos setae and gecko biomimetics.

Here, we quantified the effect of macroscale geometric protrusions on adhesive function in geckos at the level of single toes and multiple distributed toes composing a foot. We pulled single toes and whole feet attached to rods and spheres of diameters comparable to the size of the toes and feet while measuring force and varying three parameters: size, shape and orientation. Our findings not only expand our understanding of bio-attachment by providing insight into how geckos might interact with macroscale unevenness differing in shape and orientation, but pave the way toward the development of energy landscapes defining the risks and opportunities of the routes in natural terrains (Othayoth et al., 2020).

MATERIALS AND METHODS

Animals

We purchased seven geckos [*Gekko gecko* (Linnaeus 1758)] with mass of 82.3±13.4 g (mean±s.d.) from Guangxi, China, for the experiment. The animals were raised in separate cages in a 12 h:12 h light:dark cycle room, at a temperature of ∼27°C and humidity of 35–45%. The animals were fed live insects every other day and given water daily. The experiment was approved by the Jiangsu Association for Laboratory Animal Science and performed under the Guide of Laboratory Animal Management Ordinance of China. No animals were injured during the experiments.

Experimental setup

Using a force platform apparatus (Fig. 1A), we measured both shear (tangential) and normal (vertical) forces, because shear force of toes and feet of geckos may be affected by normal loads. Considering that the large size of substrate protrusions can result in offsets or misalignments between the loaded force and the principal axes of force sensor that further cause moments affecting the force measurement, we used two symmetrically placed 2D strain-gauge type force sensors (NBIT Co. Ltd, Nanjing, China) at the same time. The gauge bridges of the two sensors were in parallel so that they functioned as one, and the possible error caused by the moments mentioned above could be decreased. Physically, the two sensors were connected by using a carbon fiber enhanced plate (CFRP plate, 40×50×3 mm). The force directions of the apparatus are indicated by the red and cyan symbols (arrows, crosses and dots) in Fig. 1. Table 1 indicates the performance of the whole apparatus.

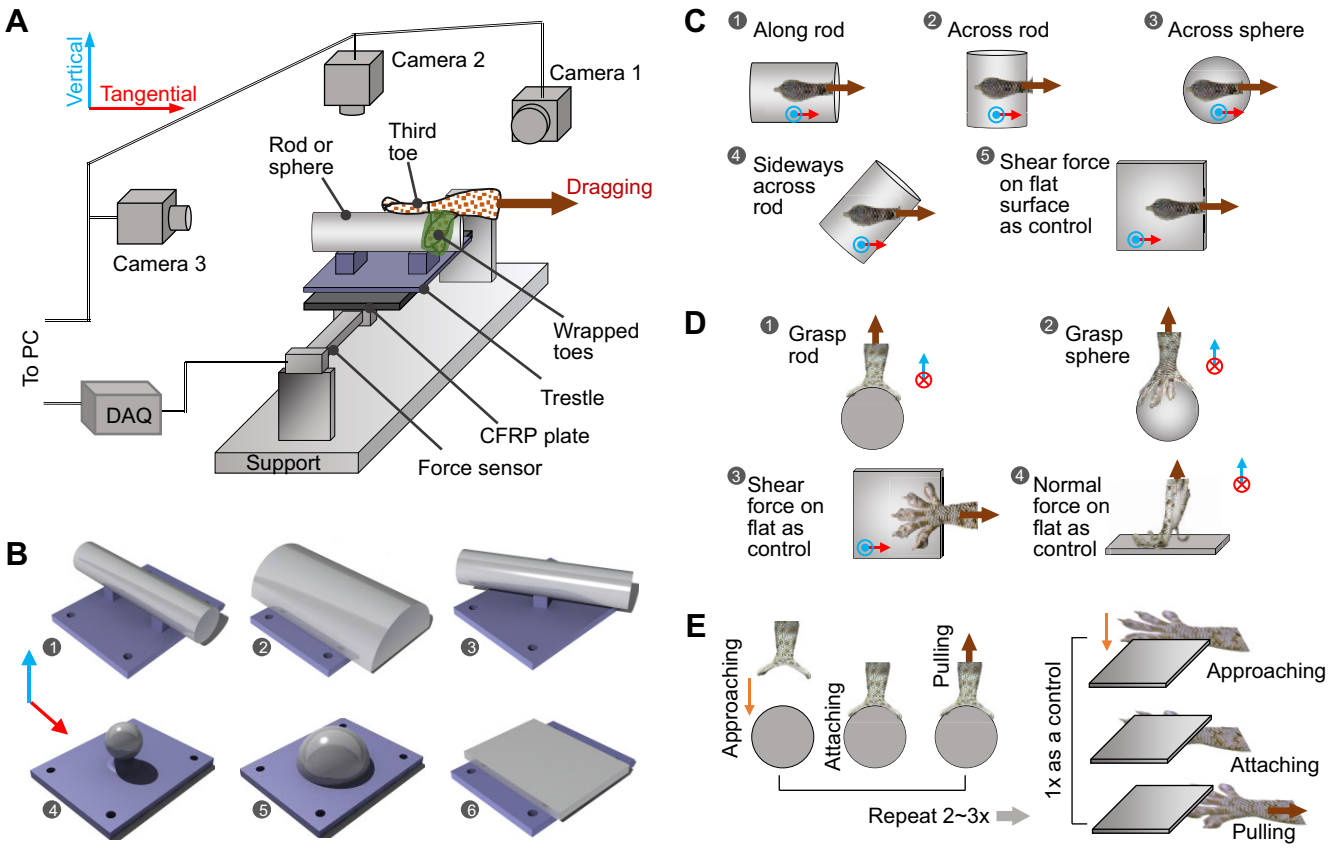

Fig. 1. Setup to measure the attachment force of single toes and whole feet of *Gekko gecko* on macro-sized substrates. (A) Experimental setup. Two parallel and symmetrical 2D force sensors were connected by using a carbon fiber enhanced plate (CFRP plate, 40×50×3 mm) so that they functioned as one. The red and cyan arrows indicate the force direction of the whole apparatus. See Table 1 for detailed calibration results. While testing the third toe of a foot, we wrapped the other toes with Teflon film. (B) Trestles were used to connect the CFRP plate and the macroscale substrate protrusion that varied in shape and diameter (1–6). (C) Tests conducted on a single toe for each condition (1–4) and a control (5). The dark brown arrows show the dragging direction, and the small red and cyan symbols indicate the direction of the measured force in the tests. (D) Tests conducted on a foot for (1) rod and (2) sphere grasping and (3) shear and (4) normal adhesion controls. The red crosses here indicate that the tangential direction is perpendicular to the paper, pointing inward, whereas the cyan dot indicates that the vertical direction here is perpendicular to the paper, pointing outward. (E) Time sequence displaying how a test was conducted.

Journal of Experimental Biology (2021) 224, jeb223438. doi:10.1242/jeb.223438

Table 1. Calibration parameters of the force-measuring apparatus

Direction	Full scale (FS)	Nonlinearity	Resolution	Coupling
Normal	20 N	0.51% FS	0.017 N	0.78% FS
Tangential	20 N	0.41% FS	0.013 N	0.60% FS

To construct macroscopically rough terrains, we mimicked macroscale protrusions of a substrate using smooth acrylic rods, spheres, semicircle rods and hemispheres with diameters ranging from 6.4 mm to 38 mm to minimize the influence of local microscale irregularity on setae attachment. To leave enough space for distributed toes of a foot to grasp the small rods and spheres (6.4 mm and 12.7 mm in diameter), we did not connect these rods and spheres with the CFRP plate directly, but used trestles manufactured by 3D printing (Fig. 1B).

Two highspeed cameras (100 frames s^{-1}, Blackfly, FLIR Systems) monitored the experiments while a NI DAQ model (SCXI1000, National Instruments) collected the force signals at 500 Hz. In the tests on toes (Fig. 1C), cameras video recorded from a lateral view (Fig. 1A, camera 1) and the top (camera 2). For feet with spread toes, we pulled them in the normal direction (Fig. 1D). In these tests, the top camera (Fig. 1A, camera 2) was moved to a tangential position (camera 3).

Tests and trial selection

Following the methods used by Gillies et al. (2014), we measured the attachment force of the third toe of a front foot or that of an entire front foot with separated, distributed toes by pulling these structures along or across rods and spheres of varying sizes (Fig. 1C,D). Fig. 1E exemplifies a complete test conducted with a foot. An individual was tested at most twice every 3 days with at least 5 h of rest between the two tests so that no animal was injured or fatigued during the experiment.

First, we measured the attachment force of the third toes of a front foot of geckos across and along rods and on spheres (Fig. 1C, 1–3). Since geckos attach to the rods and spheres on their own accord upon contact, we did not press the toes and feet toward the surface as a preload. In each test, we continuously dragged a toe 2–3 times, then pulled it on a flat acrylic sheet once as its own control (Fig. 1C, 5). The substratum was cleaned with 75% alcohol before each test. We followed these tests by measuring the attachment force on a 12.7 mm diameter rod while changing the angles between the toe and rod axis, as shown in Fig. 1C, 4. During these tests, the other toes were gently wrapped with Teflon film so that they could not touch the rods or spheres. After obtaining data from a single toe, we measured the force of the same front foot from the same individuals as they grasped the rods and spheres in the same way (Fig. 1D, 1 and 2) with both shearing and normal peeling (Fig. 1D, 3 and 4) on the flat surface as their controls.

In our experiments, the toes and feet were dragged by human hands at a random speed, which ranged from 1 to 1.5 mm s^{-1}. All the pulling was done by the same experimenter. Calculations based on the findings of Gravish et al. (2010) showed that the effect of dragging velocity on the frictional adhesion is less than 10% across the range of these velocities, so adjusting for dragging velocity as a variable when analyzing results did not affect trends or conclusions.

We used several criteria to select trials for analysis. (1) Calculations from the videos showed that the velocity of the pulling speed was within our set range. (2) For toes, the peak control force was greater than a critical value of 1 N, which was about the weight of the gecko. For feet, the critical maximum shear force on the flat surface was set as 7 N (Song et al., 2020a), and that of the normal force on the flat surface was set as 0.5 N. (3) The peak force in the direction perpendicular to dragging was less than ±1 N. Using a critical force as a benchmark, as in Gillies et al. (2014), we better standardized the data by removing alignment anomalies produced by the animal or the experimenter during the measurement.

Data processing and statistics

While pulling a toe or a foot along or across rods or spheres, the shear force developed rapidly after pulling began and decreased as the toe or foot separated from the substrate. Fig. 2 shows an example of pulling a single toe across a 25.4 mm sphere. The shear force of a single toe increased as a function of time until a near steady state was attained. We selected the maximum force for further analysis. We normalized the data relative to the maximum force from the corresponding flat control trial to minimize the possible differences caused by individual variation. The normalized value is referred to as relative force hereafter. To be simple in the following sections, the words ‘toe’ or ‘toes’ mean single toe measurements and the words ‘foot’ or ‘feet’ refer to foot experiments with multiple toes.

To determine how the macroscale rough substrate affects the adhesion of single toes and whole feet, we carried out statistical analysis for the relative force using SPSS 19.0 (IBM, USA). We used the Kruskal–Wallis (KW) test and repeated-measures ANOVA analysis with the Scheffe method for *post hoc* tests for variables of diameter (D) and toe direction (θ). A significance level of 0.05 was used throughout. In the text, the absolute force is represented as mean±s.e.m., whereas the relative force is mean±s.d.

RESULTS

Toe adhesion

The maximum force produced by a single toe for all curved surfaces ranged from 0.86 to 6.33 N (Fig. 3B,E), whereas the force on the flat control surface averaged 4.39±0.34 N (N=7 animals, n=225 measurements) (Fig. 3A,D). There was no significant relationship in control toe forces as a function of rod or sphere diameter (Fig. 3A,D; P>0.05). When we pulled the third toe of the front foot of geckos along rods whose diameter varied from 6.4 mm to 38 mm, the absolute maximum force increased from 2.13±0.56 N (N=7, n=47) on the 6.4 mm rod to 4.07±0.35 N on the 38 mm rod (Fig. 3B, green, N=7, n=48). The maximum force for across-rod pulling increased from 2.72±0.59 N (N=7, n=43) on the 6.4 mm rod to 4.45±0.52 N (N=7, n=52) on the 12.7 mm rod, then slightly decreased to 4.05±0.56 N (N=7, n=46) on the 38 mm rod (Fig. 3B). The force in across-

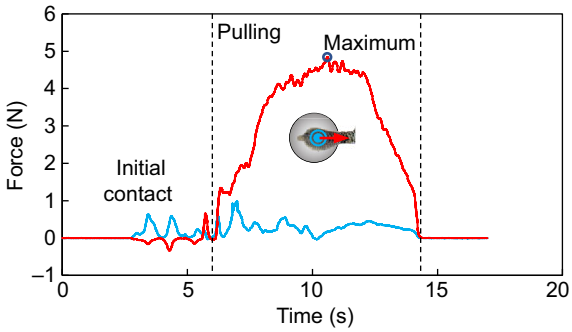

Fig. 2. Example of toe force in across-sphere pulling as a function of time. The diameter of the sphere was 25.4 mm. The whole distance of pulling is the length of the toe (~10 mm). The red line represents the shear force, while the cyan line represents the normal force. The force traces were not filtered. Data were collected at 500 Hz.

Journal of Experimental Biology (2021) 224, jeb223438. doi:10.1242/jeb.223438

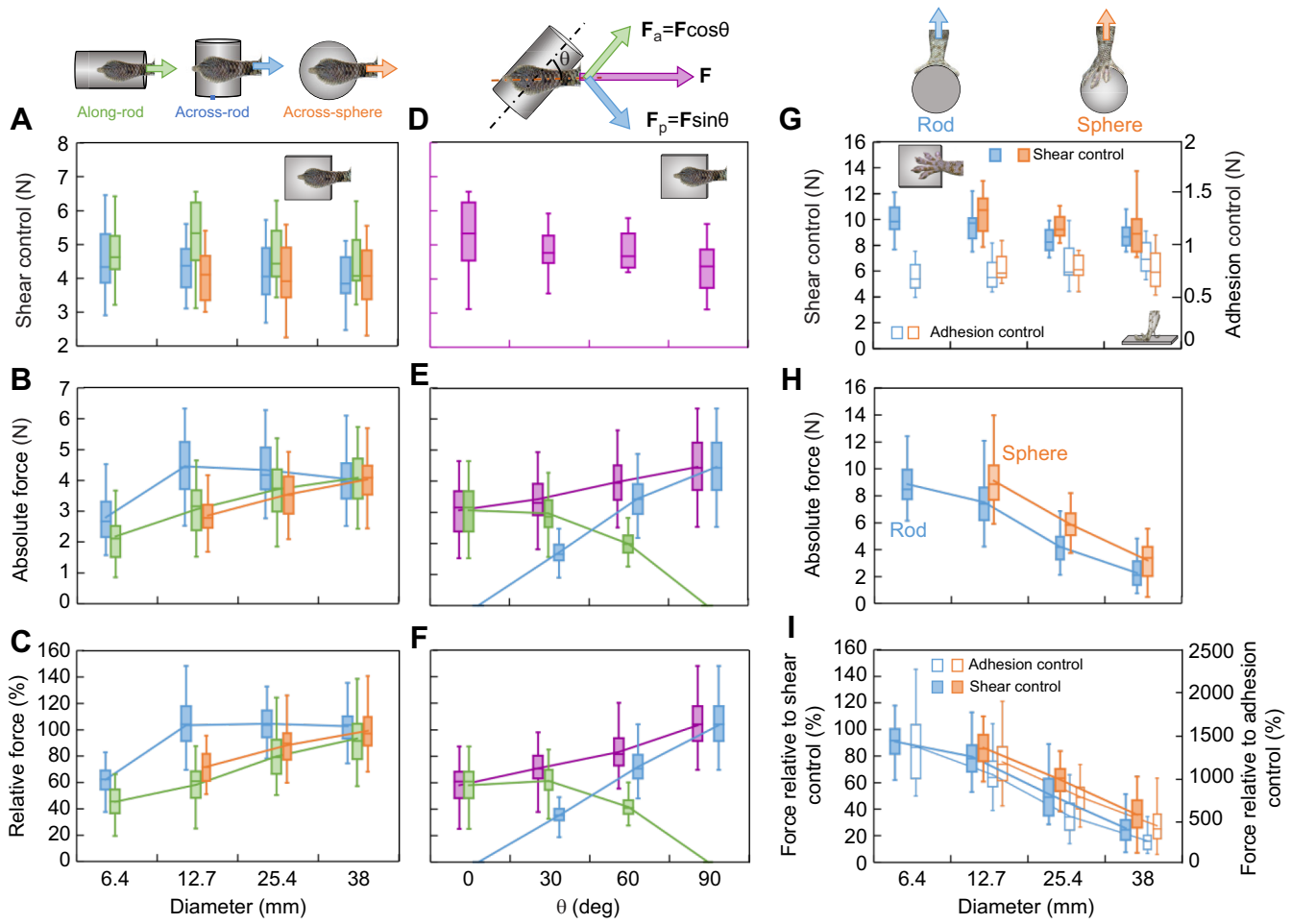

Fig. 3. Adhesion of a single toe and a whole foot on macroscale substrate features. (A–C) Forces measured for a single toe while pulled along a rod (green), across a rod (blue) and across a sphere (orange), each varying in diameter. Note that for each diameter, the forces of different substrates are plotted next to each other for clarity. Forces shown are the flat shear control (A), the absolute force (B) and the force relative to the flat shear control (C). (D–F) Forces measured for a single toe pulled on a 12.7 mm rod with changing angles (θ). The angle θ between the toe and the axis of the rod characterized the direction. The purple boxes represent the measured force (**F**, shown in the top of the middle column), the blue boxes represent the components perpendicular to the rod (i.e. $\mathbf{F_p}$=**F**sinθ, shown in the top of the middle column), and the green boxes represent the components along the rod (i.e. $\mathbf{F_a}$=**F**cosθ, shown in the top of the middle column). Relative force (in F) was calculated using the flat control (in D). (G–I) Forces of a foot, with five toes, pulled off rods (blue) and spheres (orange). The top graphic shows how force was measured. In G, the colored symbols are the maximum shear force of feet on the flat control surface, and the open symbols represent the maximum normal adhesion of feet on the flat control surface. In I, the colored symbols represent the relative force calculated by using the shear control, and the open symbols represent the relative force calculated by using the adhesion control. The top and bottom edges of boxes represent quartiles, whereas the error bars indicate maximum and minimum data points. 7 individuals were tested, and each contributed at least 6 trials.

sphere pulling (Fig. 3B, orange) increased with increasing sphere diameter similar to that for along-rod pulling, rising from 2.86 N (12.7 mm sphere, N=7, n=47) to 4.02 N (38 mm sphere, N=7, n=46). By dividing the measured curved surface forces with their corresponding flat control force, we obtained the relative force for a single toe in along-rod, across-rod and across-sphere pulling shown in Fig. 3C. The relative force of a single toe in along-rod pulling increased as the diameter of the rods increased (Fig. 3C, green; KW, χ^2=114.46, d.f.=3, P<0.001). By contrast, the attachment force of dragging toes across a rod increased from 60% on small diameter rods (6.4 mm) relative to a flat surface to 105% on larger diameter rods (12.7 mm; Fig. 3C, blue, χ^2=61.76, d.f.=1, P<0.001), but showed no further increase as rod diameter doubled (Fig. 3C, blue, χ^2=0.18, d.f.=2, P=0.9). An increase in sphere diameter also resulted in toe relative force increasing from about 70% to 98% (Fig. 3A, orange, ANOVA, $F_{2,133}$=39.93, P<0.001).

Fig. 3D–F show the results when we change the angle (θ) between the toe and the 12.7 mm rod. As θ increased from 0 deg to 90 deg, the absolute force increased from 3.04±0.58 N (θ=0 deg, N=7, n=43) to 3.41±0.39 N (θ=30 deg, N=7, n=43) and 3.97±0.35 N (θ=60 deg, N=7, n=45) before it finally reached 4.45±0.53 N (θ=90 deg, N=7, n=51). The relative force increased from 58.2±14.7% (θ=0 deg) to 105.3±19.7% (θ=90 deg), as shown in Fig. 3F (purple, χ^2=97.39, d.f.=3, P<0.001). The component of force directed perpendicular to the rod increased with angle (Fig. 3F, blue), whereas the parallel component decreased (Fig. 3F, green).

Foot adhesion

Fig. 3G–I show the results of pulling a foot possessing five soft toes differing in orientation. The maximum force for a whole foot ranged from 0.52 N to 13.96 N (Fig. 3H) in our experimental trials. The maximum shear force on the flat control surface averaged 9.38±0.42 N (N=7, n=109; Fig. 3G, solid symbols), whereas the maximum adhesion normal force pulling away from the flat control surface averaged just 0.79±0.04 N (N=7, n=109; Fig. 3G,

Journal of Experimental Biology (2021) 224, jeb223438. doi:10.1242/jeb.223438

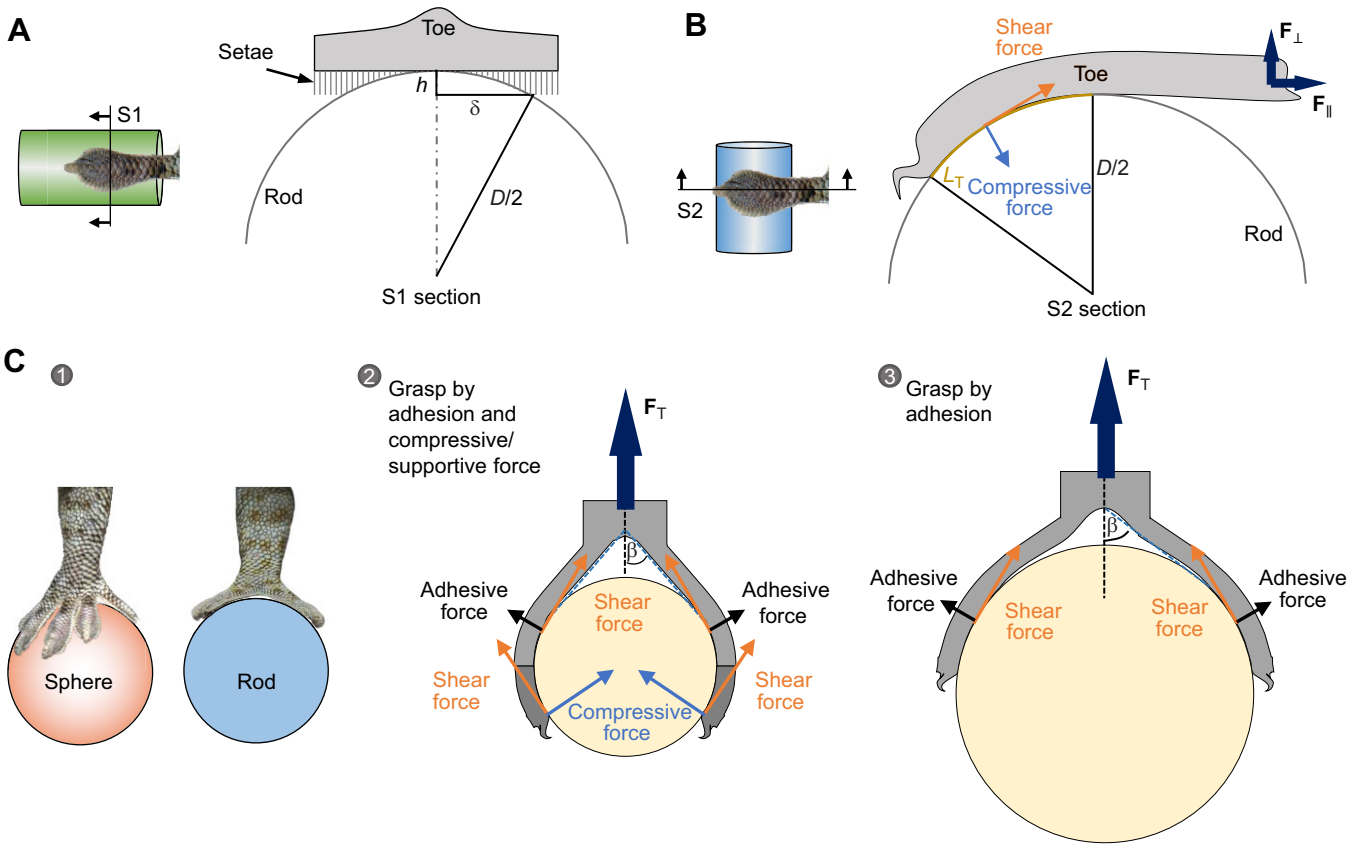

Fig. 4. Single toe and whole foot attachment hypotheses. (A) Cross-sectional view (S1) of a toe attaching to a rod along the axis of the rod. *h* is the critical depth beyond which setae will fail to touch the rod surface. δ represents the width of the available contact area for setae and is determined by the rod diameter *D* and *h*. (B) Sagittal section view (S2) of a toe attaching to a rod in the direction perpendicular to the rod axis. L_T represents the length of the contact region. (C) Typical foot–sphere and foot–rod interactions (1) in the grasp-sphere pulling and grasp-rod pulling experiments, and simple force models proposing the differences in force measured. When toes grasp a rod or sphere and are then pulled away, we hypothesize two situations: (2) On small protrusions, toes can generate perpendicular frictional adhesive forces (black arrows) and adhesion-controlled shear forces parallel to the surface (orange arrows), along with supportive wrap forces (i.e. compressive force here) supporting the object (blue arrows). The angle β represents the angle between a toe and the foot force ($\mathbf{F}_T$) direction: (3) On large protrusions, grasping likely occurs primarily by frictional adhesion (Hawkes et al., 2015) with no supportive wrap forces because the toes do not extend past the horizontal midline of the object. See Fig. S1 for further information.

open symbols). Foot forces for the flat shear control were comparable to previous reports (Irschick et al., 1996; Song et al., 2020a). There was no significant change in control foot forces as a function of rod or sphere diameter (Fig. 3G; $P>0.05$). When we pulled a foot after all toes grabbed the rod, the absolute force decreased from 8.89±0.60 N (N=7, n=42) on the 6.4 mm rod to 2.26±0.51 N (N=7, n=42) on the 38 mm rod (Fig. 3H, blue). The sphere with a diameter of 6.7 mm was too small to permit contact of a toe or foot. The pulling force on spheres also showed a decrease from 9.15±1.10 N (D=12.7 mm, N=7, n=44) to 3.24±0.69 N (D=38 mm, N=7, n=52). Fig. 3I displays the relative foot forces calculated by using a flat, shear control (solid symbols, left ordinate) and a flat, normal adhesion control (open symbols, right ordinate), respectively. Similar to the absolute force, the relative force of the foot was the greatest on the smallest rod (D=6.7 mm), attaining 90.9±13.5% of shear control force (Fig. 3I, blue solid symbols, left ordinate) and a near 15-fold increase relative to the adhesion control (open symbols; right ordinate). As the diameter of the rods increased, the relative foot force decreased from 79.5±14.4% on 12.7 mm rod to 25.7±11.4% on 38 mm rod (Fig. 3I, blue solid symbols, shear control, $F_{3,174}$=182.88, $P<0.001$). As sphere size increased, relative force decreased from 86.2±12.3% to 35.1±14.2% on the 38 mm sphere (Fig. 3I, orange, solid symbols, shear control, $F_{2,137}$=198.45, $P<0.001$). We found that relative force using the adhesive control data (open symbols; right ordinate) followed a tendency similar to that calculated using the shear control, decreasing from 1362.8±391.4% on the 6.4 mm rod to 253.7±108.6% on the 38 mm rod and from 1179.8±287.0% on the 12.7 mm sphere to 428.3±188.7% on the 38 mm sphere.

DISCUSSION

Geckos operate on natural surfaces that exhibit roughness across a large range of scales (Russell and Johnson, 2007). As pointed out by Russell et al. (2019), unscrambling the behaviors of toes and feet that facilitate the rapid locomotion of geckos remains a grand challenge, and can not only provide insight into understanding biological adhesives, but can assist in the design of gecko-inspired adhesives. Studies focused on the attachment of setae and lamellae on microscopic and mesoscopic roughness have revealed the roughness-dependent adhesion of setae and setal arrays (Gillies et al., 2014; Huber et al., 2007). Research on the whole-body performance (Vanhooydonck et al., 2005) and whole foot adhesion (Stark et al., 2015) on patterned substrates showed that the available substrate area affects foot adhesion (Russell and Johnson, 2007). In addition to the adhesive hairs, the claws also contribute significantly to interlocking with microscale irregularities (Naylor and Higham, 2019; Zani, 2000). Yet, claws can be ineffective once the size of the surface protrusion is much larger than that of the claw tips (Song

et al., 2016). Alternatively, the compliance of toes and feet can play an indispensable role when dealing with roughness at sizes similar to the lamellae (Gillies et al., 2014). Here, we show that the shape, size and orientation of the macroscale substrate features challenge the effectiveness of gecko toe and foot function.

Toe adhesion varies with the shape, size and orientation of macroscale protrusions

While interacting with the micro and nano roughness, spatulae show decreases in attachment force as the roughness (RMS) increases from 20 nm to 200 nm, but an increase when the substrate roughness increases from 200 nm to 2000 nm (Huber et al., 2007). When examining mesoscopic roughness, lamellar adhesion also displays a decrease as the size of the substrate features increase from small to lamellar size, but an increase as the size of the substrate features increase further (Gillies et al., 2014). For macroscale protrusions in our isolated toe experiments, we primarily found increases in shear force with object diameter (Fig. 3).

When we dragged a toe along round rods with diameters (D) ranging from 12.7 mm to 38 mm, the maximum relative force increased continuously and attained 95.3% of the flat control value on the 38 mm rods. Assuming all setae contribute equally, the data show that the relative force approximately scales to $D^{0.47}$($\mathbf{F}$=17.65$D^{0.47}$, R^2=0.99 for the average data; $\mathbf{F}$=17.02$D^{0.47}$, R^2=0.62 for all data), indicating the number of setae in contact might also be proportional to the 0.47 power of the rod diameter. To propose possible explanations of our results, let us assume that contacting setae fields function uniformly, even though compression of setae in the contact regions and the extent to which compliant toes will conform to the rod will require further investigation (Fig. 4A shows a cross-sectional view of an adhered toe along the rod). Let us propose a critical depth h beyond which the setae fail to contact the curved surface effectively. By assuming that toes are non-compliant in the transverse direction and considering the contact geometry (Fig. 4A, Fig. S1A), we estimated the width of contact region as $2(Dh-h^2)^{0.5}$ and contact area as $2L_T(Dh-h^2)^{0.5}$, where L_T is the length of contact region. Given that the ratio between h and D is smaller than 2.4% in our experiment, the contact area of toes along the rods changes with diameter approximately proportional to $D^{0.5}$. Thus, the shear force, which is related to the contact area (Song et al., 2020a), would be linearly related to $D^{0.5}$, approximating our experiment results. In turn, if h is specified, a critical diameter of rod on which the force will reach its plateau can be estimated. For example, if we take the setae length (about 0.11 mm) as the critical h and 4 mm as the width of a toe, we find D≈36 mm. Our results represent a first step motivating comprehensive investigation into the contact mechanics at the level of the toe and foot and, thereby, the choice of a valid contact model (e.g. Hertzian, JKR, Kendal Peel, Peel Zone; Hertz, 1881; Johnson et al., 1971; Kendall, 1975; Pesika et al., 2007; Tian et al., 2006) based on material properties and geometry of the system. We must emphasize that estimations from these simple calculations depend on the degree to which setae completely compress in the center of the contact zone, the variation in compression as rod diameter changes, and the extent of toe compliance itself. A complete mechanistic explanation of our findings requires future integration of experimentation and model validation focused on a single toe or even a part of a toe aided by advanced contact area and force measurement techniques.

If toes are precisely perpendicular to the rods, they conform to the curved surface very effectively owing to the compliance in the longitudinal direction (Russell, 1975). Measured toe forces were comparable to the flat control during perpendicular, across-rod dragging on a 12.7 mm rod (Fig. 3B, blue). Toe force did not increase further with an increase in rod diameter but remained similar to the flat control surface. Toes function effectively in the transverse direction, especially at smaller diameters, compared with along-rod pulling (Fig. 3B, green; Fig. S1A). For across-rod pulling, the toe force is determined by the length of the contact region and the local performance of setae (Fig. 4B, Fig. S1B). Generally, the shear force would be constant on most rods if no normal force is generated. As we pull a single toe, the toe seems unable to generate normal adhesive force, but likely add compressive forces as the rod diameter decreases (Fig. 4B, Fig. S1B). Presumably, as we pulled a single toe perpendicular to the rod axis, a decrease in the rod diameter seems to cause an increase in the compression to achieve a force balance in the vertical direction because the overall perpendicular forces $\mathbf{F}_\perp$ in the test were close to zero (Fig. 2). The compressive force also might function to preload the setae and can increase on small rods. A normal preload pressure can enhance setal performance (Autumn et al., 2000; Russell, 2002; Tian et al., 2006). Thus, the measured force on small rods can be theoretically larger than on flat surfaces. However, if the diameter of the rods is too small, then there will be an insufficient available surface area for the toes to contact, thus weakening the attachment (Russell and Johnson, 2007; Stark et al., 2013).

Considering that substrates often are not ideally aligned for toes, we varied the angle (θ) between the toe and a 12.7 mm rod (Fig. 1C, 4). After measuring the resultant force ($\mathbf{F}$) for a changing θ, we further computed the components along the rod axis ($\mathbf{F}_a$) and perpendicular to the rod axis ($\mathbf{F}_p$) by using $\mathbf{F}_a$= $\mathbf{F}$cosθ and $\mathbf{F}_p$= $\mathbf{F}$sinθ, respectively (Fig. 3E,F). Interestingly, with the increase in angle (θ), the component perpendicular to the rod increased consistently ($\mathbf{F}_p$=1.175θ, R^2=0.99 for average data; $\mathbf{F}_p$=1.164θ, R^2=0.96 for all data), whereas the component along the rod decreased when the angle was smaller than 30 deg, with the greatest decrease at a 60 deg angle ($\mathbf{F}_a$=−0.012θ^2+0.416θ+58.206, R^2=0.99 for average data, $\mathbf{F}_a$=−0.013θ^2+0.473θ+58.261, R^2=0.86 for all data). Consequently, the shear force of toes increased moderately when the angle was smaller than 60 deg with the greatest increase occurring at 90 deg.

Spheres seem to possess both the advantages and disadvantages speculated for rods. Toes can bend longitudinally to fit the round surface to possibly produce compressive forces. Yet, toes likely fail to contact effectively widthwise due to the curvature of substrate. We found that attachment capability of toes on spheres was reduced in comparison with across-rod pulling, but was more similar to along-rod pulling, especially when the sizes of spheres were intermediate at 12.7–25.4 mm (Fig. 3B, orange).

Our findings indicated that the size, shape and orientation of the macroscale protrusion on a substrate affect the toe's adhesive force significantly. However, even though the toe may realize only 50% of its adhesive potential on a rod whose diameter corresponds to the width of a toe, the absolute force (about 2 N) is still large enough to hold a whole gecko weighing 100 g.

Foot adhesion varies with the shape, size and orientation of macroscale protrusions

For feet, both the absolute and relative force increased as the diameter of rods and spheres decreased. The force on the smallest diameter sphere (12.7 mm; 9.15±1.11 N) was the largest measured in all our experiments. Although a toe can display about 60% of its potential while being pulled perpendicularly across a rod (6.4 mm; Fig. 3C blue), a foot with five toes grasping the same rod, with toes nearly perpendicular to the rod, generated the largest force

(8.89±0.60 N) for this shape (Fig. 3H and Fig. 4C, 2). Our results support the findings of Hawkes et al. (2015), who designed a remarkably effective gecko-inspired, shear adhesion gripper that uses fibrillar adhesives to conform to rods, spheres, and a variety of shapes.

Morphological observations indicate that feet, with their controllable, distributed, compliant toes are able to conform to, and even grasp the macro-scale rough substrates when geckos negotiate a series of vertical rods during sideways wall running (Song et al., 2020a), more like that observed in chameleons (Spinner et al., 2014) and human hands (Sundaram et al., 2019). By doing this, feet successfully reverse the force tendencies observed in toes for protrusion size, generating large forces on small protrusions.

To begin to explain our force measurements using morphological observations (Fig. 4C, 1), we illustrate two possible foot behaviors (Fig. 4C, 2 and 3). Toes could partially wrap around and grasp small protrusions (Fig. 4C, 2), but are unable to wrap very large objects (Fig. 4C, 3). For small objects, toes wrapping under the horizontal midline can generate perpendicular compressive forces toward the object, thereby supporting it (Fig. 4C, blue arrows), while being pulled. Friction caused by the above-mentioned compression can expand the grasping potential of feet, but is not always required because of the existence of the adhesive force perpendicular to and away from the object's surface results from the frictional adhesion produced by setae (Fig. 4C, black arrows; Autumn et al., 2006b; Hawkes et al., 2015). Notably, active adduction may occur among the distributed toes and could create an extra perpendicular, squeeze-induced force pushing the object away to create a normal reaction force that increases the shear force tangential to the object. Unfortunately, it is almost impossible to distinguish how much the active adduction contributed to local compression, thereby the shear force, in the recent experiments. We thus did not make a strict distinction here and treated them as one for a general discussion. Frictional adhesion couples the perpendicular force to the shear force parallel to the surface (Fig. 4C, orange arrows; see Fig. S1 for more detail).

For both cases, assuming all toes function equally, we can approximate the total force ($\mathbf{F}_T$) of a foot containing five toes (Fig. 4C) using:

$$\mathbf{F}_T = 5(\mathbf{F}_{\parallel}\cos\beta \pm \mathbf{F}_{\perp}\sin\beta), \quad (1)$$

where β is the angle between a toe and the final force direction, and $\mathbf{F}_{\parallel}$ and $\mathbf{F}_{\perp}$ are the overall parallel and perpendicular forces of a single toe originating at the point of toe separation from the object, respectively (the plus or minus sign depends on the direction of $\mathbf{F}_{\perp}$; see Fig. S1 for details). If the perpendicular forces ($\mathbf{F}_{\perp}$) of the toes are negligible, Eqn 1 becomes comparable to the form used by Hawkes et al. (2015) (see their eqn 1).

Generally, on large rods and sphere protrusions where β was close to 90 deg, dragging was mainly resisted by the adhesive force, whereas on small diameter protrusions where β was less than 90 deg, the shear force of toes contributed more. Therefore, with the decrease in β, the source of the measured force shifted from the perpendicular force ($\mathbf{F}_{\perp}$) to the parallel force $\mathbf{F}_{\parallel}$. As the parallel force was generally much greater than the perpendicular force at toes, this provides a partial explanation for feet developing large forces on small rods and spheres. Also, through the synergistic function among toes, feet expand the adhesive regions of toes and add the capability of exerting grasping supportive forces. By considering the frictional adhesion law of setae (Autumn et al., 2006b) and assuming that the local compressive force is not larger than the local shear force, we explored Eqn 1 and equations mentioned in Fig. S1C for the aim of maximizing $\mathbf{F}_T$, and found that although squeezing forces that increase the normal force, and thereby friction (which is a component of local parallel force), are possible, generating shear force and attractive force at all toes is likely beneficial for feet adhering to large protrusions (Fig. 4C, 3; Fig. S1C3; and also as shown in Hawkes et al., 2015), whereas generating compressive (supportive) force at the bottom part of toes (refer to the horizontal axis of protrusion with adhesion at the upper part of toes) will facilitate foot attachment to small protrusions (Fig. 4C2, Fig. S1C3) which can be wrapped by toes. When compression occurs, the pressure might produce more intimate contact of the setal arrays, and, therefore, larger forces than behaviors without a preload. Feet also allow the toes to wrap the protrusions more completely. Consequently, one may expect an increase in total force for any single toe in this case. This could partly explain why a single toe develops only about 60% of its shear adhesion when being pulled perpendicular to a 6.4 mm rod (Fig. 3C, blue), but multiple toes permit foot forces to attain over 90% of the shear control on that same, small diameter rod (Fig. 3I, blue solid symbols). As mentioned above, active adduction might occur during the experiment and enhance the performance of toes, and thereby that of the whole foot, but this is hard to clarify here as adduction is quite complex in a gecko foot possessing five toes and may also be dependent on the substrate. Although technically challenging, synchronous measurement of individual toe force and EMG of all five toes during grasping would be a useful next step.

A final important finding demonstrates the importance of shape. Relative force of feet on spheres was greater than that on rods with the same diameter (Fig. 3I, D=12.7 mm, $F_{1,87}$=5.57, P=0.02; D=25.4 mm, $F_{1,83.78}$=14.10, P<0.001; D=38 mm, $F_{1,92}$=14.59, P<0.001). A foot can only distribute five toes to the two sides of the rod while grasping the rod but can spread toes to span more contact area when grasping a sphere (Fig. 4C, 1). Thus, some toes will not be perpendicular to the axis of the rods and will fail to reach their maximum adhesive force when grasping rods (Fig. 3F). By contrast, all toes can attach along the tangential direction of surface at the contact region while grasping spheres.

Foot and toe function at the macroscale – a bridge to the natural environment

Our results point to the high adaptability of feet containing multiple compliant toes. In addition to geckos with adhesive toes, other animals with distributed toes (or fingers) also exhibit the capability of grasping objects similar in size to the toes themselves (Krause and Fischer, 2013; Marzke and Wullstein, 1996; Schmidt and Fischer, 2010). Adding compliance and grasping to multiple, distributed (i.e. separable) toes significantly increases the capability of effective interactions with surfaces composed of macroscale features. Since the natural environment is often full of features similar in size to animal attachment devices, such as tree branches, rough tree bark and rocks (Russell and Johnson, 2007), toes can be highly advantageous. Moreover, the ability to realign toes during rapid running when encountering a perturbation adds to the effectiveness (Song et al., 2020a). The design of foot attachment using distributed toes has also proved successful in enhancing the climbing ability of legged robots (Kim et al., 2007). Incorporating compliance and controllability of multiple, distributed toes to accommodate the terrain where robots must operate will further increase their capacity to interact with a range of macroscale rough shapes in their environment.

The exceptional adhesive capability of gecko toes and feet results in the extraordinary rapid, reliable and reversible attachment required for agile locomotion on a wide array of terrains in any orientation. Here, we quantified how the shape, size and orientation of the macroscale features of the substrate affect toe and foot adhesive force production by affecting the available contact areas, the curvature of a toe and the configuration of toes on the foot. Feet consisting of multiple compliant toes can generate sufficient force under the most challenging circumstances in our experiment by taking advantage of the adjustable distributed control. Results not only increase our understanding of the gecko attachment on the macroscale rough substrate, but also provide bio-inspiration for manufacturing the feet of climbing robots by using distributed, soft and controllable toes.

Acknowledgements
We thank Kellar Autumn, Hannah Stuart and Elliot Hawkes for providing expertise on adhesion and grasping. Zhouyi Wang and Andrew Saintsing offered useful comments to improve the manuscript.

Competing interests
The authors declare no competing or financial interests.

Author contributions
Conceptualization: Y.S., Z.D., R.J.F.; Methodology: Y.S., J.Y., L.Z., Z.D., R.J.F.; Software: Y.S.; Validation: Y.S., J.Y., L.Z.; Formal analysis: Y.S.; Investigation: Y.S., J.Y., L.Z.; Resources: Y.S., J.Y.; Data curation: Y.S., Z.D., R.J.F.; Writing - original draft: Y.S., J.Y., L.Z., Z.D., R.J.F.; Writing - review & editing: Y.S., J.Y., L.Z., Z.D., R.J.F.; Visualization: Y.S., Z.D., R.J.F.; Supervision: Z.D., R.J.F.; Project administration: Z.D., R.J.F.; Funding acquisition: Z.D., R.J.F., Y.S.

Funding
This research was supported by the National Natural Science Foundation of China to Z.D. (51435008), University of California, Berkeley Institutional Funds to Center for interdisciplinary Bio-inspiration in Education and Research (CiBER) to R.J.F., a scholarship from the China Scholarship Council to Y.S.

References
Abdala, V., Manzano, A. S., Tulli, M. J. and Herrel, A. (2009). The tendinous patterns in the palmar surface of the lizard manus: functional consequences for grasping ability. *Anat. Rec.* **292**, 842-853. doi:10.1002/ar.20909

Alexander, R. M. (2003). *Principles of Animal Locomotion*. Princeton University Press.

Autumn, K., Liang, Y. A., Hsieh, S. T., Zesch, W., Chan, W. P., Kenny, T. W., Fearing, R. and Full, R. J. (2000). Adhesive force of a single gecko foot-hair. *Nature* **405**, 681-685. doi:10.1038/35015073

Autumn, K., Hsieh, S. T., Dudek, D. M., Chen, J., Chitaphan, C. and Full, R. J. (2006a). Dynamics of geckos running vertically. *J. Exp. Biol.* **209**, 260-272. doi:10.1242/jeb.01980

Autumn, K., Dittmore, A., Santos, D., Spenko, M. and Cutkosky, M. (2006b). Frictional adhesion: a new angle on gecko attachment. *J. Exp. Biol.* **209**, 3569-3579. doi:10.1242/jeb.02486

Chen, J. J., Peattie, A. M., Autumn, K. and Full, R. J. (2006). Differential leg function in a sprawled-posture quadrupedal trotter. *J. Exp. Biol.* **209**, 249-259. doi:10.1242/jeb.01979

Dai, Z., Gorb, S. N. and Schwarz, U. (2002). Roughness-dependent friction force of the tarsal claw system in the beetle Pachnoda marginata (Coleoptera, Scarabaeidae). *J. Exp. Biol.* **205**, 2479-2488.

Daltorio, K. A., Gorb, S. N., Peressadko, A., Horchler, A. D., Ritzmann, R. E. and Quinn, R. D. (2006). A robot that climbs walls using micro-structured polymer feet. In *Climbing and Walking Robots* (ed. M. O. Tokhi, G. S. Virk and M. A. Hossain), pp. 131-138. Berlin Heidelberg, German: Springer.

Ge, L., Sethi, S., Ci, L., Ajayan, P. M. and Dhinojwala, A. (2007). Carbon nanotube-based synthetic gecko tapes. *Proc. Natl. Acad. Sci. USA* **104**, 10792-10795. doi:10.1073/pnas.0703505104

Gillies, A. G., Henry, A., Lin, H., Ren, A., Shiuan, K., Fearing, R. S. and Full, R. J. (2014). Gecko toe and lamellar shear adhesion on macroscopic, engineered rough surfaces. *J. Exp. Biol.* **217**, 283-289. doi:10.1242/jeb.092015

Gorb, S., Varenberg, M., Peressadko, A. and Tuma, J. (2007). Biomimetic mushroom-shaped fibrillar adhesive microstructure. *J. R. Soc. Interface* **4**, 271-275. doi:10.1098/rsif.2006.0164

Gravish, N., Wilkinson, M., Sponberg, S., Parness, A., Esparza, N., Soto, D., Yamaguchi, T., Broide, M., Cutkosky, M., Creton, C. et al. (2010). Rate-dependent frictional adhesion in natural and synthetic gecko setae. *J. R. Soc. Interface* **7**, 259-269. doi:10.1098/rsif.2009.0133

Hawkes, E. W., Christensen, D. L., Han, A. K., Jiang, H., Cutkosky, M. R. (2015). Grasping without squeezing: Shear adhesion gripper with fibrillar thin film. In 2015 IEEE International Conference on Robotics and Automation (ICRA), pp. 2305-2312. Seattle, WA, USA. doi:10.1109/ICRA.2015.7139505

Hertz, H. (1881). *On the Contact of Elastic Solids*, *J. Reine. Angew Math.* **92**,156-171.

Higham, T. E. and Jayne, B. C. (2004). Locomotion of lizards on inclines and perches: hindlimb kinematics of an arboreal specialist and a terrestrial generalist. *J. Exp. Biol.* **207**, 233-248. doi:10.1242/jeb.00763

Higham, T. E., Russell, A. P., Niewiarowski, P. H., Wright, A. and Speck, T. (2019). The ecomechanics of gecko adhesion: natural surface topography, evolution, and biomimetics. *Integr. Comp. Biol.* **59**, 148-167. doi:10.1093/icb/icz013

Huber, G., Gorb, S. N., Hosoda, N., Spolenak, R. and Arzt, E. (2007). Influence of surface roughness on gecko adhesion. *Acta Biomater.* **3**, 607-610. doi:10.1016/j.actbio.2007.01.007

Irschick, D. J., Austin, C. C., Petren, K., Fisher, R. N., Losos, J. B. and Ellers, O. (1996). A comparative analysis of clinging ability among pad-bearing lizards. *Biol. J. Linn. Soc.* **59**, 21-35. doi:10.1111/j.1095-8312.1996.tb01451.x

Johnson, K. L., Kendall, K. and Roberts, A. D. (1971). Surface energy and the contact of elastic solids. *Proc. R. Soc. A Math. Phys. Sci. Eng. Sci.* **324**, 301-313. doi:10.1098/rspa.1971.0141

Kaspari, M. and Weiser, M. (2007). The size–grain hypothesis: do macroarthropods see a fractal world? *Ecol. Entomol.* **32**, 279-282. doi:10.1111/j.1365-2311.2007.00870.x

Kendall, K. (1975). Thin-film peeling-the elastic term. *J. Phys. D. Appl. Phys.* **8**, 1449-1452. doi:10.1088/0022-3727/8/13/005

Kim, S., Spenko, M., Trujillo, S., Heyneman, B., Mattoli, V. and Cutkosky, M. R. (2007). Whole body adhesion: Hierarchical, directional and distributed control of adhesive forces for a climbing robot. In Proceedings 2007 IEEE International Conference on Robotics and Automation, pp. 1268-1273. Roma, Italy.

Krause, C. and Fischer, M. S. (2013). Biodynamics of climbing: effects of substrate orientation on the locomotion of a highly arboreal lizard (Chamaeleo calyptratus). *J. Exp. Biol.* **216**, 1448-1457. doi:10.1242/jeb.082586

Marzke, M. W. and Wullstein, K. L. (1996). Chimpanzee and human grips: a new classification with a focus on evolutionary morphology. *Int. J. Primatol.* **17**, 117-139. doi:10.1007/BF02696162

Menon, C. and Sitti, M. (2006). A biomimetic climbing robot based on the gecko. *J. Bionic Eng.* **3**, 115-125. doi:10.1016/S1672-6529(06)60015-2

Naylor, E. R. and Higham, T. E. (2019). Attachment beyond the adhesive system: the contribution of claws to gecko clinging and locomotion. *Integr. Comp. Biol.* **59**, 168-181 doi:10.1093/icb/icz027

Niewiarowski, P. H., Dhinojwala, A. and Garner, A. M. (2019). A physical model approach to gecko adhesion opportunity and constraint: how rough could it be? *Integr. Comp. Biol.* **59**, 203-213. doi:10.1093/icb/icz029

Othayoth, R., Thoms, G. and Li, C. (2020). An energy landscape approach to locomotor transitions in complex 3D terrain. *Proc. Natl. Acad. Sci. USA* **117**, 14987-14995. doi:10.1073/pnas.1918297117

Pesika, N. S., Tian, Y., Zhao, B., Rosenberg, K., Zeng, H., McGuiggan, P., Autumn, K. and Israelachvili, J. N. (2007). Peel-zone model of tape peeling based on the gecko adhesive system. *J. Adhes.* **83**, 383-401. doi:10.1080/00218460701282539

Pillai, R., Nordberg, E., Riedel, J. and Schwarzkopf, L. (2020). Nonlinear variation in clinging performance with surface roughness in geckos. *Ecol. Evol.* **10**, 2597-2607. doi:10.1002/ece3.6090

Qu, L., Dai, L., Stone, M., Xia, Z. and Wang, Z. L. (2008). Carbon nanotube arrays with strong shear binding-on and easy normal lifting-off. *Science* **322**, 238-242. doi:10.1126/science.1159503

Ruibal, R. and Ernst, V. (1965). The structure of the digital setae of lizards. *J. Morphol.* **117**, 271-293. doi:10.1002/jmor.1051170302

Russell, A. P. (1975). A contribution to the functional analysis of the foot of the Tokay, Gekko gecko (Reptilia: Gekkonidae). *J. Zool.* **176**, 437-476. doi:10.1111/j.1469-7998.1975.tb03215.x

Russell, A. P. (1981). Descriptive and functional anatomy of the digital vascular system of the tokay, Gekko gecko. *J. Morphol.* **169**, 293-323. doi:10.1002/jmor.1051690305

Russell, A. P. (2002). Integrative functional morphology of the gekkotan adhesive system (Reptilia: Gekkota). *Integr. Comp. Biol.* **42**, 1154-1163. doi:10.1093/icb/42.6.1154

Russell, A. P. and Bellairs, D. (1976). Some comments concerning interrelationships amongst gekkonine geckos. In *Morphology and Biology of Reptiles* (ed. A. d. A. Bellairs and C. B. Cox), pp. 217-244. London: Academic Press.

Russell, A. P. and Higham, T. E. (2009). A new angle on clinging in geckos: incline, not substrate, triggers the deployment of the adhesive system. *Proc. R. Soc. B Biol. Sci.* **276**, 3705-3709. doi:10.1098/rspb.2009.0946

Russell, A. P. and Johnson, M. K. (2007). Real-world challenges to, and capabilities of, the gekkotan adhesive system: contrasting the rough and the smooth. *Can. J. Zool.* **85**, 1228-1238. doi:10.1139/Z07-103

Russell, A. P. and Johnson, M. K. (2014). Between a rock and a soft place: microtopography of the locomotor substrate and the morphology of the setal fields of Namibian day geckos (Gekkota: Gekkonidae: Rhoptropus). *Acta Zool.* **95**, 299-318. doi:10.1111/azo.12028

Russell, A. P., Stark, A. Y. and Higham, T. E. (2019). The integrative biology of gecko adhesion: historical review, current understanding, and grand challenges. *Integr. Comp. Biol.* **59**, 101-116. doi:10.1093/icb/icz032

Schmidt, A. and Fischer, M. S. (2010). Arboreal locomotion in rats - the challenge of maintaining stability. *J. Exp. Biol.* **213**, 3615-3624. doi:10.1242/jeb.045278

Sitti, M. and Fearing, R. S. (2003). Synthetic gecko foot-hair micro/nano-structures as dry adhesives. *J. Adhes. Sci. Technol.* **17**, 1055-1073. doi:10.1163/156856103322113788

Song, Y., Dai, Z., Wang, Z., Ji, A. and Gorb, S. N. (2016). The synergy between the insect-inspired claws and adhesive pads increases the attachment ability on various rough surfaces. *Sci. Rep.* **6**, 26219. doi:10.1038/srep26219

Song, Y., Dai, Z., Wang, Z. and Full, R. J. (2020a). Role of multiple, adjustable toes in distributed control shown by sideways wall-running in geckos. *Proc. R. Soc. B Biol. Sci.* **287**, 20200123. doi:10.1098/rspb.2020.0123

Song, Y., Lu, X., Zhou, J., Wang, Z., Zhang, Z. and Dai, Z. (2020b). Geckos distributing adhesion to toes in upside-down running offers bioinspiration to robots. *J. Bionic Eng.* **17**, 570-579. doi:10.1007/s42235-020-0045-0

Spinner, M., Westhoff, G. and Gorb, S. N. (2014). Subdigital setae of chameleon feet: friction-enhancing microstructures for a wide range of substrate roughness. *Sci. Rep.* **4**, 5481. doi:10.1038/srep05481

Stark, A. Y., Badge, I., Wucinich, N. A., Sullivan, T. W., Niewiarowski, P. H. and Dhinojwala, A. (2013). Surface wettability plays a significant role in gecko adhesion underwater. *Proc. Natl. Acad. Sci. USA* **110**, 6340-6345. doi:10.1073/pnas.1219317110

Stark, A. Y., Palecek, A. M., Argenbright, C. W., Bernard, C., Brennan, A. B., Niewiarowski, P. H. and Dhinojwala, A. (2015). Gecko adhesion on wet and dry patterned substrates. *PLoS ONE* **10**, e0145756-e0145756. doi:10.1371/journal.pone.0145756

Sundaram, S., Kellnhofer, P., Li, Y., Zhu, J.-Y., Torralba, A. and Matusik, W. (2019). Learning the signatures of the human grasp using a scalable tactile glove. *Nature* **569**, 698-702. doi:10.1038/s41586-019-1234-z

Tian, Y., Pesika, N., Zeng, H., Rosenberg, K., Zhao, B., McGuiggan, P., Autumn, K. and Israelachvili, J. (2006). Adhesion and friction in gecko toe attachment and detachment. *Proc. Natl. Acad. Sci. USA* **103**, 19320-19325. doi:10.1073/pnas.0608841103

Unver, O., Uneri, A., Aydemir, A. and Sitti, M. (2006). Geckobot: A gecko inspired climbing robot using elastomer adhesives. In Proceedings 2006 IEEE International Conference on Robotics and Automation, pp. 2329-2335. Orlando, FL, USA.

Vanhooydonck, B., Andronescu, A., Herrel, A. and Irschick, D. J. (2005). Effects of substrate structure on speed and acceleration capacity in climbing geckos. *Biol. J. Linn. Soc.* **85**, 385-393. doi:10.1111/j.1095-8312.2005.00495.x

Wang, Z., Wang, J., Ji, A., Zhang, Y. and Dai, Z. (2011). Behavior and dynamics of gecko's locomotion: the effects of moving directions on a vertical surface. *Chin. Sci. Bull.* **56**, 573-583. doi:10.1007/s11434-010-4082-7

Wang, Z., Dai, Z., Ji, A., Ren, L., Xing, Q. and Dai, L. (2015). Biomechanics of gecko locomotion: The patterns of reaction forces on inverted, vertical and horizontal substrates. *Bioinspir. Biomim.* **10**, 016019. doi:10.1088/1748-3190/10/1/016019

Zani, P. A. (2000). The comparative evolution of lizard claw and toe morphology and clinging performance. *J. Evol. Biol.* **13**, 316-325. doi:10.1046/j.1420-9101.2000.00166.x

Zhuang, M. V. and Higham, T. E. (2016). Arboreal Day Geckos (Phelsuma madagascariensis) differentially modulate fore- and hind limb kinematics in response to changes in habitat structure. *PLoS ONE* **11**, e0153520. doi:10.1371/journal.pone.0153520